II. PLASMA DYNAMICS

A. PLASMA PHYSICS*

Prof. S. C. Brown	D. E. Baldwin	J. J. McCarthy
Prof. W. P. Allis	C. D. Buntschuh	W. J. Mulligan
Prof. D. J. Rose	S. Frankenthal	J. J. Nolan, Jr.
Prof. D. R. Whitehouse	R. B. Hall	R. J. Papa
Dr. G. Bekefi	M. O. Harwit	Judith S. Vaughen
Dr. Magda Ericson	J. L. Hirshfield	C. S. Ward
Dr. S. Gruber	W. R. Kittredge	S. Yoshikawa

1. HEAT TRANSPORT IN PLASMAS

In Quarterly Progress Report No. 56 (pages 21-25), we discussed the spatial decay of the electron temperature T and of the electron density n along the z-axis of a plasma column that was heated at one end and immersed in an axial dc magnetic field B. We obtained the following differential equation for the variation of T with z:

$$\frac{d^2\underline{U}}{dz_o^2} - \frac{d\underline{U}}{dz_o} = \gamma\left[1 - \frac{1}{\underline{U}}\right] \tag{1}$$

subject to the boundary conditions: $\underline{U} = \underline{U}_{max}$, at $z = 0$; and $\underline{U} \to 1$, $d\underline{U}/dz_o \to 0$ as $z_o \to \infty$. Here $\underline{U} = U/U_e$; U is the mean energy, 3/2 kT, of an electron; and U_e is the equilibrium energy to which the electron decays at an infinite distance z from the region of excitation. The dimensionless parameter z_o is equal to βz, where β is the reciprocal of the free diffusion length in the radial direction of the plasma cylinder, given by

$$\beta = (2.405/R)\left(1+\mu_-^2 B^2\right)^{-1/2} \tag{2}$$

where R is the radius of the plasma column, and μ_- is the electron mobility. We assume, now, that a transition to the ambipolar limit is made by writing Eq. 2 as $(2.405/R)\left(1+\mu_+\mu_- B^2\right)^{-1/2}$. The constant γ of Eq. 1 is given by

$$\gamma = \frac{9}{10}\,\frac{mG\nu_c^2}{\beta^2 U_e} \tag{3}$$

where m is the electron mass, ν_c is the electron collision frequency for momentum transfer, and $(G\nu_c)$ is the fractional energy loss per electron per second. Equation 3 contains those parts of the coefficient of thermal conduction K which are independent

*This work was supported in part by the Atomic Energy Commission under Contract AT(30-1)-1842; in part by the Air Force Cambridge Research Center under Contract AF 19(604)-5992; and in part by National Science Foundation under Grant G-9930.

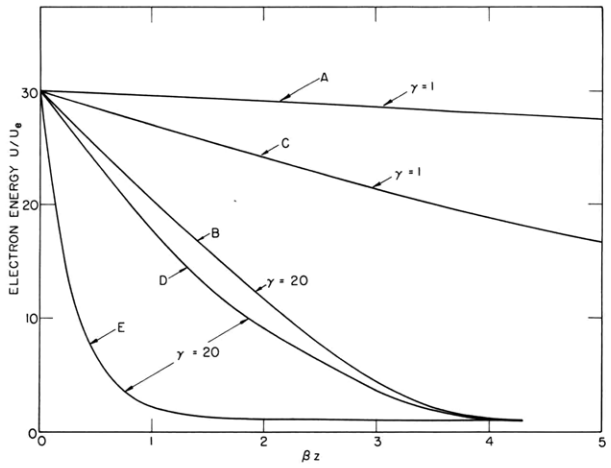

Fig. II-1. Variation of electron energy with distance along the plasma column.

of U and n. When ν_c is independent of electron velocity, the tensor component of K for heat flow in the z direction is

$$K = \frac{10}{3} \frac{knU_e}{m\nu_c} \tag{4}$$

The assumptions made in deriving Eq. 1 are: (a) Outside the excitation region $z > 0$, no fields, other than the dc magnetic field, act on the plasma. (b) No excitation or ionization takes place in the region $z > 0$, and the only loss of electrons is by diffusion. (c) There are no temperature gradients in the radial direction r. Nevertheless, there is transport of energy in both the r and z directions. The variation in the energy density is given by

$$nU = (nU)_{max} J_o(2.405r/R) \exp(-\beta z) \tag{5}$$

(d) The energy density decays in the lowest diffusion mode, as exemplified by Eq. 5. (e) The charged-particle diffusion coefficient is directly proportional to the electron temperature. For this to be true, the electron temperature must greatly exceed that of the ion temperature.

Curves A and B of Fig. II-1 are solutions of Eq. 1, showing the variation of U with z, for $\gamma = 1, 20$. For given values of ν_c and U_e, the larger the γ, the lower the loss of particles to the radial walls. This is achieved either by increasing R or B, or both. Curves C and D represent the results when electron diffusion is neglected. The differential equation appropriate to this case is

$$\frac{d}{dz_o} \underline{U} \frac{d\underline{U}}{dz_o} = \frac{1}{2} \gamma(\underline{U}-1) \tag{6}$$

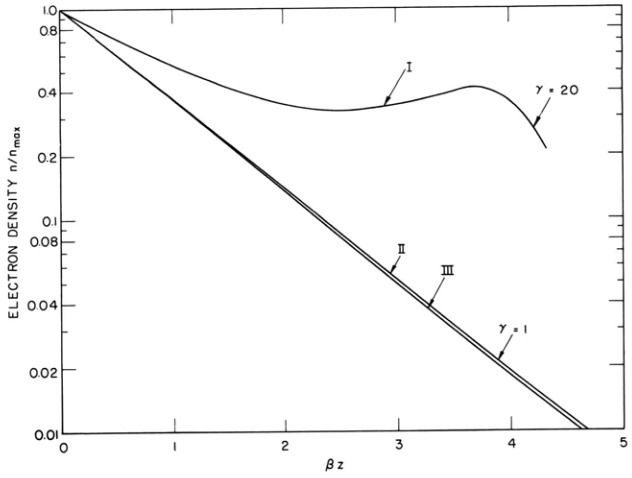

Fig. II-2. Variation of electron density with distance along the plasma column.

We note that when γ is large (diffusion is small), the error involved in neglecting particle loss is not serious (compare curves B and D). However, when γ is small, diffusion must not be neglected (compare curves A and C). Curve E shows what happens when diffusion is neglected, and when the coefficient of thermal conduction is assumed to be a constant (as is sometimes done) and equal to $(10\ knU_e/3m\nu_c)$.

The spatial variation of the electron density in the presence of thermal gradients can be obtained from Eq. 5, by using the values of U from curves A and B of Fig. II-1. The results are shown by curves I and II of Fig. II-2. These curves are to be compared with curve III, in which the effects of temperature gradients on the decay of the electron density are neglected. When the temperature gradients are small (γ=1), they influence the density variations only slightly. But when the energy decays quickly (γ=20), the hot electrons diffuse more rapidly to the radial walls than the cold electrons, with the consequence that the decay of electron density is inhibited (curve I). For large values of βz (not shown in Fig. II-2), the slope of curve I approaches asymptotically the slope of curve III.

G. Bekefi

2. A MICROWAVE RADIATION PYROMETER

The incoherent microwave noise that emanates from a plasma can be used in the determination of its radiation temperature T. This determination is generally made by a direct application of Kirchhoff's radiation law,

$$P_\omega = B(\omega, T)\, A_\omega \tag{1}$$

where P_ω is the emission in the radian frequency interval between ω and $\omega + d\omega$; $B(\omega, T)$

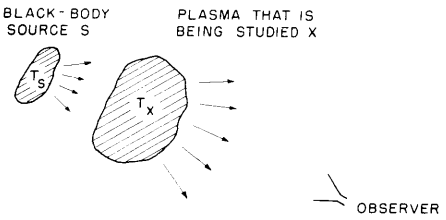

Fig. II-3. Illustrating the observation of noise emission from an unknown plasma illuminated by a black-body source.

is the black-body emission; and A_ω is the power absorption coefficient of the plasma. Since A_ω, for a plasma of arbitrary properties, is not generally known and is difficult to measure accurately, and A_ω can range from almost zero value (when the plasma hardly radiates) to unity (when it radiates like a black body), the evaluation of T, from Eq. 1, raises serious problems.

This note describes a technique of measuring T that does not require a knowledge of A_ω. The principle of the technique (1, 2) may be described as follows: The plasma that is being studied (henceforth, denoted X) is illuminated by a source of black-body radiation (denoted S) of variable temperature T_S. An observer views the black-body radiation S through the unknown plasma X, as shown in Fig. II-3. As T_S is varied, a point is reached when the intensity seen by the observer is independent of the presence or absence of the plasma X. This is the case when the temperature T_X of X is just equal to T_S because, now, X absorbs as much power from S as it radiates in the direction of the observer. A more quantitative argument shows that this result is independent of A_ω. The emission from S is $B(\omega, T_S)$. A fraction $(1-A_\omega)$ of this radiation is absorbed in its passage through X. The total emission P_T in the direction of the observer is, therefore,

$$P_T = (1-A_\omega)\, B(\omega, T_S) + A_\omega B(\omega, T_X)$$

When X is turned off, the change in intensity, ΔP_ω, seen by the observer is

$$\Delta P_\omega = (1-A_\omega)\, B(\omega, T_S) + A_\omega B(\omega, T_X) - B(\omega, T_S)$$

or it may be rewritten as

$$\Delta P_\omega = A_\omega [B(\omega, T_S) - B(\omega, T_X)] \qquad (2)$$

When $T_S = T_X$ no change in intensity is observed, irrespective of the value of A_ω. This is also true for inhomogeneous and anisotropic plasmas.

In our qualitative discussion we have omitted effects caused by reflection and scattering of energy from plasma X. Note, also, that to achieve the necessary variations of $B(\omega, T_S)$ in any practical system, it may be necessary to interpose absorbing bodies between the two plasmas. These bodies themselves radiate, and their radiation must not be neglected.

Consider the arrangement shown in Fig. II-4 which bears directly on the experimental system that will be described. Both plasmas (S and X) are situated in a waveguide, one end of which is terminated by a matched load, and the other connected to a

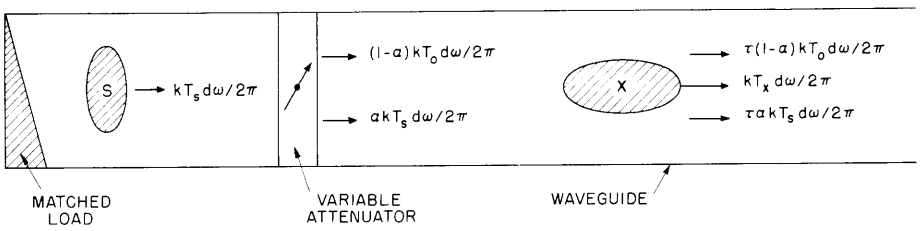

Fig. II-4. Waveguide analogue of Fig. II-3.

receiver. An attenuator (of variable attenuation α) is placed between the two plasmas. For convenience in this discussion, the waveguide is assumed to propagate only one mode. The power radiated along the waveguide (3) by the black body S is given by

$$P_{\omega S} = kT_S d\omega/2\pi \text{ watts} \tag{3}$$

This power is reduced by the attenuation α of the attenuator. The total power, $P_{\omega\alpha}$, leaving the attenuator is

$$P_{\omega\alpha} = \alpha kT_S d\omega/2\pi + (1-\alpha)\, kT_o d\omega/2\pi \tag{4}$$

The last term in Eq. 4 represents the power radiated by the attenuator, which is assumed to be at room temperature T_o. A fraction $\tau_\omega P_{\omega\alpha}$ of the power incident on X is transmitted through it; τ_ω is the power transmission coefficient of X and is related to the absorption coefficient A_ω and the power reflection coefficient Γ_ω through the relation

$$1 = A_\omega + \tau_\omega + \Gamma_\omega \tag{5}$$

The total power $P_{\omega T}$ leaving plasma X (as observed at some distance along the waveguide where any higher evanescent modes have died down) is, from Eqs. 1, 4, and 5,

$$P_{\omega T} = (kd\omega/2\pi)\,[A_\omega T_X + \{1-\Gamma_\omega - A_\omega\}\,\{\alpha T_S + (1-\alpha)T_o\}] \tag{6}$$

When the plasma X is turned off, A_ω of Eq. 6 equals zero, and Γ_ω changes to a new value Γ'_ω, where Γ'_ω is the reflection coefficient of the vessel which contains plasma X. Adjusting α until $P_{\omega T}$ of Eq. 6 remains the same irrespective of the presence or absence of X, we obtain

$$T_X = \alpha T_S \left[1 - \frac{1-\alpha}{\alpha}\frac{T_o}{T_S}\right]\left[1 + \frac{\Delta\Gamma_\omega}{A_\omega}\right] \tag{7}$$

where $\Delta\Gamma_\omega = \Gamma_\omega - \Gamma'_\omega$.

From Eq. 7, therefore, it is evident that the present method of measuring T_X is limited to those cases for which $\Delta\Gamma_\omega \ll A_\omega$, that is, when the reflections from the plasma

are small compared with its absorption. This is not a very serious limitation. When the plasma is very dense (that is, when it occupies a great length of waveguide, or when the charge concentration is high), $\tau = 0$, $A_\omega = (1-\Gamma_\omega)$, and T_X can be determined from the known value of α and from a measurement of Γ (obtained from a measurement (3) of the VSWR of a signal incident on X). On the other hand, when the plasma is very tenuous (low charge concentration), it can be shown that $\Delta\Gamma_\omega$ varies approximately as the fourth power of the ratio of plasma frequency to radian frequency, $\omega_p/\omega = \left(ne^2/m\epsilon_o\omega\right)^{1/2}$, whereas A_ω varies as the square of ω_p/ω. Hence, at sufficiently low electron densities n, or at sufficiently high measuring frequencies ω, $\Delta\Gamma_\omega/A_\omega$ can always be made sufficiently small compared with unity; and there is only the relatively small region between the dense and transparent plasma where measurements of T_X require a knowledge of A_ω.

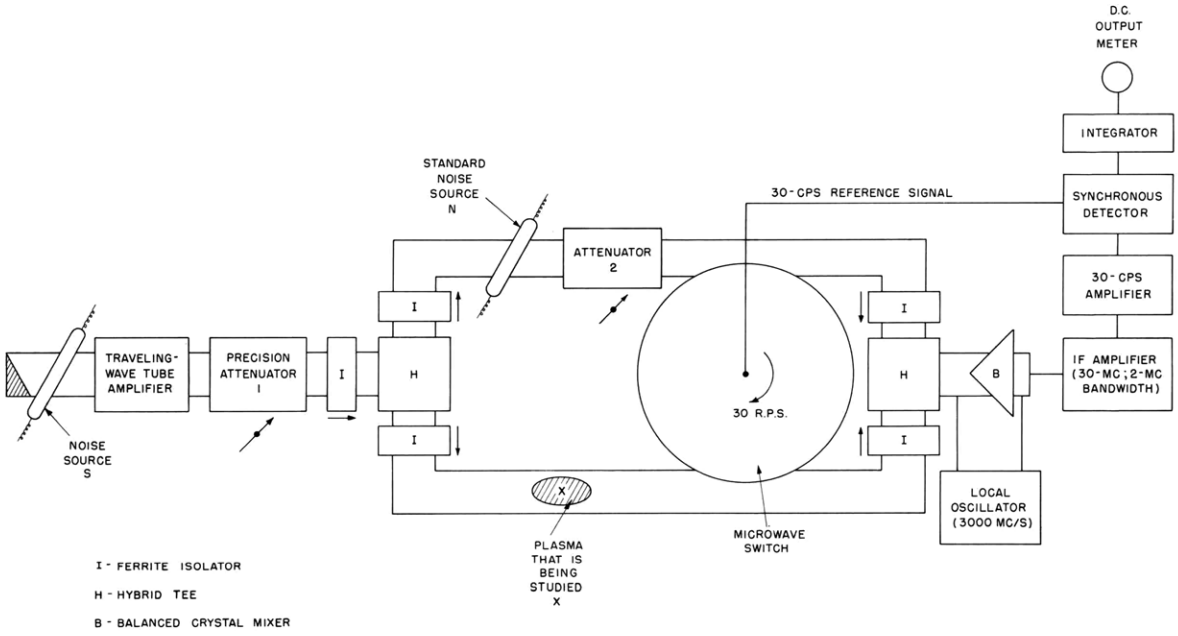

Fig. II-5. Schematic diagram of experimental apparatus.

The experimental apparatus is shown in Fig. II-5. The power from the noise source S $\left(T_S \approx 10^4 °K\right)$ is amplified with a wideband traveling-wave tube that has a gain of 20 db. This amplification is necessary when T_X exceeds T_S. The power from the traveling-wave tube is varied by means of a precision attenuator. The output from the attenuator is split into approximately two halves. One half is used to illuminate the plasma X. The other half serves as a noise reference. The power traveling along the two channels is compared periodically (3) thirty times in a second. With plasma X turned off, the power in the two channels is equalized by adjusting attenuator 2, until a null is observed

on the dc output meter. Plasma X is then turned on, and precision attenuator 1 is adjusted for a null output. The reading, a, of this attenuator determines T_X of Eq. 7, in terms of the equivalent noise temperature T_S from the traveling-wave tube. Every so often, T_S is calibrated absolutely in terms of T_N, the black-body noise standard N situated in the upper channel. This is done by turning X off, turning N on, and adjusting precision attenuator 1 to a new reading, a', for a null output reading. Then, T_X is given by

$$T_X = \frac{a}{a'} T_N \left[1 - \frac{1 - a}{a} \frac{T_o}{T_S} \right]$$

The temperature T_X can be measured with an accuracy of ±100°K.

Measurements of the temperature of the positive column of a dc discharge immersed in a static, axial magnetic field are now being made.

G. Bekefi

References

1. F. A. Jenkins and H. E. White, Fundamentals of Physical Optics (McGraw-Hill Book Company, New York, 1937), p. 261.

2. A. L. Gilardini, Technical Note No. 1, Contract AF61(052)-39, Air Force Cambridge Research Center, Bedford, Massachusetts, August 1959.

3. G. Bekefi, J. L. Hirshfield, and S. C. Brown, Phys. Rev. 116, 1051 (1959).

3. RADIOFREQUENCY CONFINEMENT IN THE PRESENCE OF MAGNETIC HILLS

The main limitation on the effectiveness of a magnetic hill, for confinement purposes, is the unavoidable leakage of particles whose velocities lie nearly parallel to the magnetic field. A method of reflecting these particles is considered in this report. The basic technique was originally proposed by Vedenov and his coworkers (1). They suggested employing a high-frequency magnetic field at right angles to the dc field, for the purpose of converting the particle energy that is parallel to the magnetic field into perpendicular energy.

Without giving a detailed derivation here, the time-averaged force on a charged particle caused by the dc magnetic-field gradients is

$$\bar{f} = (\bar{\mu} \cdot \nabla) \bar{B}_o \tag{1}$$

where B_o is the dc magnetic field, and $\bar{\mu}$ is the magnetic moment defined by

$$\bar{\mu} = \frac{q}{2} \langle \bar{r} \times \bar{v} \rangle \tag{2}$$

If we assume that an rf magnetic field of the form

$$\left.\begin{aligned} B_x &= B_x \sin \Omega t \\ B_y &= B_y \sin (\Omega t+\phi) \end{aligned}\right\} \tag{3}$$

is present, then the magnetic moment defined by Eq. 2 can be computed. Such an analysis, under the condition that $B_o \gg B_x$, leads to

$$\mu_z = -\left[\frac{1}{2}\left(\frac{mv_\perp^2}{B_o}\right) - \frac{1}{2}\left(\frac{mv_{||}^2}{B_o}\right) R \sin \phi\right] \tag{4}$$

where $v_\perp$ and $v_{||}$ are velocities perpendicular and parallel to the magnetic field. The parameter R is defined as

$$R = \left(\frac{\omega_{bx}\omega_{by}}{\omega_B \Omega}\right) \tag{5}$$

The first term in Eq. 5 is the usual magnetic moment associated with a particle in a magnetic field. The second term arises because the ac magnetic field deflects the parallel motion of the particles into transverse motion. In order for the second term to aid in the reflection properties from magnetic hills, it is necessary that $\sin \phi < 0$, which means that the magnetic field rotates in the same direction as the natural orbit of the charged particle.

In order to assess the importance of the "extra" magnetic moment indicated in Eq. 4, it is necessary to examine the magnitude of R. For a laboratory of our size, B_o is limited to approximately 1000 gauss, and B_x to approximately 100 gauss. In this case, the parameter, R_e, for electrons, is

$$R_e = \frac{1.76 \times 10^8}{\Omega} \tag{6}$$

Since R is inversely dependent on mass, calculations for ions will be neglected.

The maximum frequency that can be used in such a system can be approximately determined by setting R = 1. Then, both $v_{||}$ and $v_\perp$ have equal weight in determining the magnetic moment. We have

$$\Omega_{max} = 1.76 \times 10^8 \text{ rad/sec} \tag{7}$$

The minimum frequency that can be used can be estimated by requiring that the particle spend enough time in the high-frequency field so that the time averages calculated in evaluating the force given by Eq. 1 are valid. A crude estimate of this minimum frequency may be obtained by setting the rf period equal to (L/v_o), where L and v_o

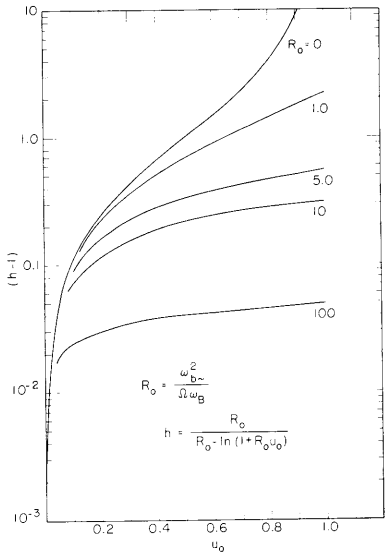

Fig. II-6. Magnetic hill required for reflection (U_o is the ratio of parallel to total energy).

represent the length over which the ac field acts, and the initial velocity, respectively. If the length L is 10 cm, and the electron has an energy of 10 ev, then Ω_{min} will be 1.2×10^8 rad/sec. By comparing the minimum and maximum frequencies, we find that the usable frequency range is rather narrow. In order to obtain a more precise estimate of the minimum frequency, an analysis of the particle motion must be made.

From Eqs. 1 and 4, the motion parallel to the dc magnetic field can be analyzed. The solution for the parallel energy in terms of the magnetic field is

$$U = \frac{1}{R}\left\{-1+(1+U_o R_o)\exp\left[-R_o\left(1-\frac{B_o}{B}\right)\right]\right\} \tag{8}$$

where $U = \left(v_{\parallel}^2\right)\Big/\left(v_o^2\right)$, and B_o is the initial magnetic field. The magnetic-hill ratio is determined by setting U equal to zero. Thus

$$h = \frac{R_o}{R_o - \ln(1+R_o U_o)} \tag{9}$$

As we expected, the energy depends only on the magnetic field — not on the variation of the field. The hill ratio h is shown in Fig. II-6, plotted against the initial parallel energy. It is obvious that the most severe requirements occur when the initial velocity lies entirely along the magnetic field. The maximum hill ratio h_{max} thus occurs for $U_o = 1$. This curve is shown in Fig. II-7.

It is still necessary to determine the time, t_r, which is required for the parallel

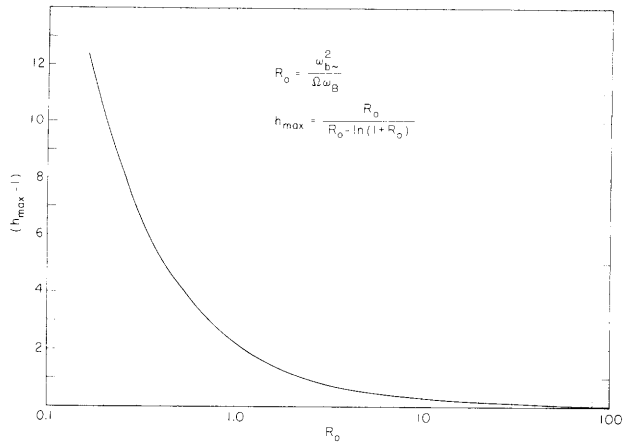

Fig. II-7. Maximum hill ratio required for reflection.

velocity to be reduced to zero. This time, obviously, depends on how the magnetic field varies with distance and, for simplicity, it will be chosen to be

$$B = B_o\, e^{\alpha z} \tag{10}$$

In this case, the approximate equation of motion is

$$\frac{dx}{d\tau} = -\frac{1}{2}\left(1+(R_{av}-1)x^2\right) \tag{11}$$

where $x = (v_{||})/(v_o)$, $\tau = \alpha v_o t$, and R_{av} is the average value of R (averaged with respect to the magnetic field). Equation 11 is only approximately correct because (R-1) is replaced by $(R_{av}-1)$. The solution of Eq. 11 is well known (2), and leads to the time τ_r that is required to reduce the parallel velocity to zero. This information is plotted in Fig. II-8, from which Ω_{min} can be determined.

It is necessary to compare the magnetic-hill force that has been discussed here with the rf confining force that is proportional to the gradients of the ac electric field. Although the analysis is not presented here, the force on a charged particle which results from a circularly polarized magnetic field is

$$f_z = \frac{\frac{1}{2}\frac{q^2}{m}\frac{d}{dz}B^2}{\mu_o\epsilon_o\left(\omega_p^2+\Omega\omega_b\right)} \tag{12}$$

If the electron density is very low, the particle energy that can be reflected is determined approximately, from Eq. 12, to be

$$U = R_o\,\frac{1}{2}\,\frac{mc^2}{e} \tag{13}$$

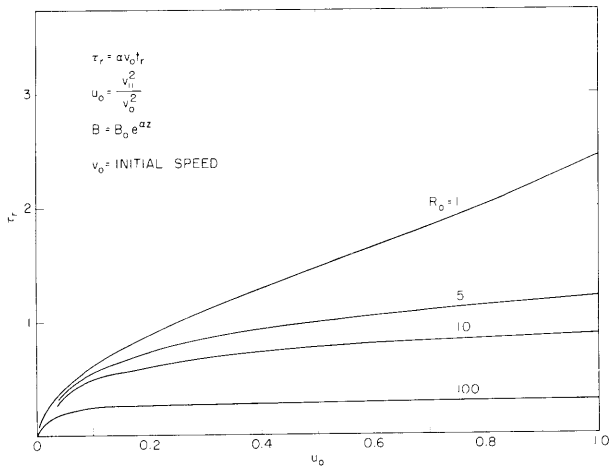

Fig. II-8. Normalized time, τ_r, required for reflection versus fraction of energy parallel to the dc magnetic field.

For the numerical values previously chosen, this energy is indeed very large. Thus with $R_o = 1$, the energy U is found to be 2.5×10^5 ev. This might, at first, seem sufficient to reflect almost all particles. It is necessary to consider, however, what happens in a practical device. If we assume a density of 10^{11} in the ac field region and a dc magnetic field of B = 1000 gauss, the electron energy that can be reflected is reduced by a large amount. For $\Omega = 10^8$, the energy given by Eq. 13 should be reduced by a factor of approximately 200. This reduction in the reflected energy is caused by the shielding of the electric field by the plasma. Of course, this effect becomes more important at higher densities.

In summary, it may be stated that the presence of a magnetic hill in conjunction with a circularly polarized magnetic field will be of extreme importance when rf confinement is attempted on dense plasmas.

R. B. Hall

References

1. A. A. Vedenov, T. V. Volkov, L. I. Rudakov, and R. Z. Sagdeyev, Thermal insulation and confinement of plasma with a high-frequency electromagnetic field (theory), United Nations Peaceful Uses of Atomic Energy, Proc. Second International Conference, Geneva, September 1958, Vol. 32, pp. 239-243 (1958).

2. R. S. Burington, Handbook of Mathematical Tables and Formulas (Handbook Publishers, Inc., Sandusky, Ohio, 3rd ed., 1949), p. 64.

4. ELECTROSTRICTION IN PLASMAS

It is well known that a plasma in alternating fields can be regarded as a dielectric medium; many of the results that are valid for dielectrics are applicable to plasmas.

In particular, there exist electrostriction effects; that is, a plasma placed in an electric field may expand or contract. These effects are highly intensified in a low-density plasma because of its high compressibility.

A plasma can be treated as a dielectric because the total amount of energy stored has the same expression that it has in a dielectric, $(KE^2)/(8\pi)$ per unit volume (in cgs units), where E is the electric field, and K is the dielectric constant of the plasma. For, the work performed by the electric field per unit time, $\vec{E} \cdot \vec{j}$, where $\vec{j}$ is the current, may be written

$$\vec{E} \cdot \vec{J} = \vec{E} \cdot \chi \frac{\partial \vec{E}}{\partial t} = \frac{\partial}{\partial t}\left[\frac{1}{2}\chi E^2\right]$$

with the notation $\vec{j}_E$, the projection of the current on the electric field vector, $\vec{j}_E = \chi(\partial\vec{E}/\partial t)$. In the absence of collisions, χ is real; $(\chi/2)(E^2)$ represents reversible work, which can be entirely recovered. The total energy stored is given by

$$\frac{E^2}{8\pi} + \frac{1}{2}\chi E^2 = \frac{KE^2}{8\pi} \qquad K = 1 + 4\pi\chi$$

If there are collisions, one part of the work performed by the electric field is dissipated into irreversible Joule heating; the other part, which is reversible, is $\frac{\partial}{\partial t}\left[\frac{1}{2}\chi_r E^2\right]$, where χ_r is the real part of χ, and the energy stored is $\left(K_r E^2\right)/(8\pi)$. Therefore, the steady forces that compress or expand the plasma are obtained in the same way as they are for a dielectric.

We consider a plasma in a form of an infinite slab, placed in an alternating electric field $\vec{E}$ of frequency ω. ($\vec{E}$ is the electric field vector of a standing wave and is perpendicular to the slab.) There is a steady magnetic field B parallel to the slab. (See Fig. II-9.) We assume that the thickness ℓ of the plasma is small compared with the wavelength, so that in the absence of plasma the magnitude of the electric field does not vary over the distance ℓ. We also assume that the magnitude of the electric field is a slowly varying function of the coordinates, so that the effect of the alternating magnetic field is negligible.

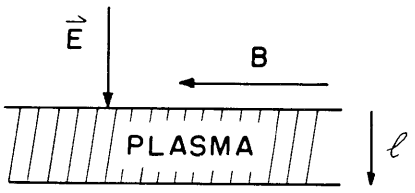

Fig. II-9. Illustrating the geometry of the plasma and the configuration of the fields.

We consider 1 cm^2 of the slab. The plasma consists of N electrons and N ions per cm^2 of surface. We want to calculate the volume, V_o, occupied by these charged particles in the steady state; to do this, we must annul the total force acting on the plasma.

We make the following assumptions: The ions have an infinite mass; the plasma

has an infinitely sharp boundary; the density is uniform inside the plasma; the temperature T of the electrons is larger than the temperature T_i of the ions and is such that the drift energy of the electrons is small compared with their thermal energy (cgs units are used). The normal force resulting from the electric field, which tends to compress or expand the plasma, is $(-\partial/\partial\ell)$ W, where W is the change in energy caused by the presence of the plasma.

$$W = -\frac{E_o^2}{8\pi} V + \frac{KE_p^2}{8\pi} V$$

where E_p is the electric field inside the plasma. Because of the continuity of the normal component of $K\vec{E}$, $E_p = E_o/K$; and W becomes

$$W = \frac{1 - K}{K} \frac{E_o^2}{8\pi} V$$

The force that reacts against the compression of the plasma is due to the decrease in entropy when the plasma is compressed. There may also be Coulomb forces because the interior of the plasma is not strictly neutral, since there are surface charges; but we neglect these forces. The total force acting on the plasma is zero when $-\partial/\partial\ell[W-TS] = 0$. This procedure is equivalent to finding the minimum with respect to the volume of W - TS, which is the free energy of the system. Because of the existence of an irreversible process, the procedure of minimization of the free energy is not strictly correct; the problem should be treated by a minimum entropy production procedure.

We have assumed the drift energy of the electrons to be small compared with their thermal energy. In this case, the electric field only slightly perturbs the distribution function for the electrons; that is, we may consider the distribution isotropic, with a Maxwellian distribution for the velocities, and take for the entropy of the electrons that of a perfect gas. The volume-dependent part of the free energy therefore becomes

$$\frac{1 - K}{K} \frac{E_o^2}{8\pi} V - NkT \log V$$

which has to be minimized with respect to the volume.

In the absence of collisions, the dielectric constant K is given by $K = 1 + \frac{\omega_p^2}{\omega_b^2 - \omega^2}$, where $\omega_b = eB/m$ is the cyclotron frequency associated with the dc magnetic field; and ω_p is the plasma frequency related to the density n of electrons by

$$\omega_p^2 = \frac{4\pi ne^2}{m} = \frac{4\pi e^2}{m} \frac{N}{V} = \frac{\Omega_p^2}{V}$$

where $\Omega_p^2 = (4\pi Ne^2)/n$. The term W becomes

$$W = -\frac{E_o^2}{8\pi} \frac{V}{V \frac{\omega_b^2 - \omega^2}{\Omega_p^2} + 1}$$

If $\omega < \omega_b$, the term W is a decreasing function of the volume, and there is no finite minimum for the free energy. If $\omega > \omega_b$, this term has a discontinuity for $V_o = \frac{\Omega_p^2}{\omega^2 - \omega_b^2}$ and varies with V as indicated in Fig. II-10.

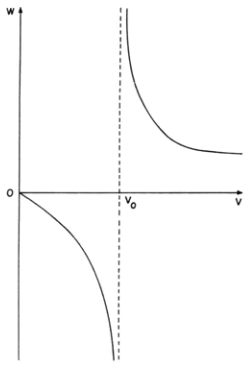

Fig. II-10. Variation of W, the change in energy caused by the presence of the plasma, with the volume of the plasma.

If we introduce collisions, they smooth the discontinuity, and the negative infinity is replaced by a deep minimum which occurs for a volume close to V_o. The other term for the free energy, -TS, is a decreasing function of the volume that, in principle, shifts the minimum toward larger volumes. If the temperature T is not too high, the shift will be very small. We can neglect the term -TS in finding the minimum if the slope of the curve W at the point V_o is greater than the slope of the curve -TS at the same point. This condition is given by $\frac{E_o^2}{8\pi} \frac{\omega^2 - \omega_b^2}{\nu_1^2} > \frac{NkT}{V_o}$, where ν_1 is the collision frequency. If the volume offered to the plasma is infinite, the absolute minimum occurs for an infinite volume because NkT log V becomes infinite when V becomes infinite; V_o represents a metastable state. But we are considering the case in which the volume of the walls containing the plasma is sufficiently small, so that V_o is an absolute minimum for this volume.

The relation $V_o = \frac{\Omega_p^2}{\omega^2 - \omega_b^2}$ which is found when $\omega > \omega_b$ may also be written $\omega_p^2 = \omega^2 - \omega_b^2$. If the total number, N, of electrons inside the plasma is changed (all other

conditions remaining the same), the plasma adjusts its volume to keep a constant density so that $\omega_p^2 = \omega^2 - \omega_b^2$.

These results can be extended to a cylindrical geometry. The dc magnetic field is axial in the z direction and the ac electric field, E_o, in the absence of plasma is uniform and perpendicular to the axis, in the x direction. The change in energy because of the presence of the plasma is

$$W = \frac{1 - K}{8\pi} \int \vec{E}_o \vec{E}_p \, dv$$

Here, $\vec{E}_p$ is the electric field inside the plasma, and the integration is performed over the volume of the plasma. In the absence of a steady magnetic field, $\vec{E}_p = \frac{2\vec{E}_o}{1 + K}$ and $W = \frac{2E_o^2}{8\pi} \frac{1 - K}{1 + K}$. The discontinuity in the W term occurs for K = -1, or $\omega_p^2 = 2\omega^2$. In the presence of a dc magnetic field, the electric field inside the plasma is uniform but is no longer parallel to $\vec{E}_o$. It is given (1) by

$$E_x = \frac{2(1+K_T)}{(1+K_T)^2 + K_H^2} E_o$$

$$E_y = \frac{2K_H}{(1+K_T)^2 + K_H^2} E_o$$

where $K_T = 1 + \frac{\omega_p^2}{\omega_b^2 - \omega^2}$ is the dielectric coefficient in the x direction, and $K_H = j \frac{\omega_p^2}{\omega_b^2 - \omega^2} \frac{\omega_b}{\omega}$ is the Hall dielectric coefficient. The discontinuity in W occurs for $\omega_p^2 = 2\omega(\omega - \omega_b)$. If ω_b is close to ω, this expression is equivalent to $\omega_p^2 = \omega^2 - \omega_b^2$, which was found for plane geometry.

Table II-1.

B (gauss)	$(\omega - \omega_b)$ (gauss)	ω_p^2 (measured)	ω_p^2 (calculated)
900	128	7.5×10^{19}	10.2×10^{19}
920	108	6.3×10^{19}	8.6×10^{19}
940	88	4.7×10^{19}	7×10^{19}
960	68	4.1×10^{19}	5.4×10^{19}
980	48	3.6×10^{19}	3.9×10^{19}

The results of this theory are in agreement with experimental results obtained by C. S. Ward (2) for a cylindrical geometry with an axial magnetic field. In Table II-1 we compare the measured values of ω_p^2 with the predicted values for ω_p^2, $2\omega(\omega-\omega_b)$.

Magda Ericson

References

1. S. J. Buchsbaum, Private communication (by letter, March 1960).

2. C. S. Ward, Private communication, Massachusetts Institute of Technology, January 1960.

5. MAGNETOAMBIPOLAR DIFFUSION

Recent papers (1, 2) concerning the diffusion of an ambipolar plasma in a magnetic field have shown that it is possible to have unequal electron and ion currents flowing to specific regions of a container with a zero net electric current over the whole container. These unbalanced currents arise from the anisotropic behavior of the plasma in a magnetic field, but predictions as to their magnitude have been confused by the seeming importance of the boundary conditions. It is shown here that for an active plasma, metal boundaries are a necessary condition for accomodating unbalanced currents in the steady state, but the ionization frequency in the volume of the plasma is a sufficient condition for determining their magnitude.

The following description of the plasma in a magnetic field uses the macroscopic current equations derived from Boltzmann transport theory

$$\overline{\Gamma}_\pm \mp \mu_\pm \overline{\Gamma}_\pm \times \overline{B} = \pm \mu_\pm n \overline{E} - \overline{\nabla}(D_\pm n) \tag{1}$$

where $\overline{\Gamma}_+$ and $\overline{\Gamma}_-$ are the ion and electron particle current densities; μ_+ and μ_- are the ion and electron mobilities; D_+ and D_- are the ion and electron diffusion coefficients in the neutral background gas; $\overline{B}$ is the static applied magnetic field; $\overline{E}$ is the resultant space-charge field, and n is the electron or ion density because they are equal for large densities ($n=n_+=n_-$). Using cylindrical geometry, with the z-axis along the magnetic field, we can write the vector equations (Eqs. 1) in their component form. Assuming cylindrical symmetry with $E_\theta = 0$ and $\frac{\partial n}{\partial \theta} = 0$, we obtain for the θ-component equations

$$\Gamma_{\pm\theta} = \mp \mu_\pm \Gamma_{\mp r} B \tag{2a}$$

Using these equations to eliminate Γ_θ in the r-component equations, we get

$$\Gamma_{\pm r} = \pm b_\pm \mu_\pm n E_r - b_\pm D_\pm \frac{\partial n}{\partial r} \tag{2b}$$

For the z-component, we have

$$\Gamma_{\pm z} = \pm\mu_{\pm} n E_z - D_{\pm} \frac{\partial n}{\partial z} \tag{2c}$$

In Eq. 2b the quantity b, called the magnetic quenching factor, is defined as

$$\text{ion quenching factor } b_+ = \frac{1}{1 + \mu_+^2 B^2} \tag{3a}$$

$$\text{electron quenching factor } b_- = \frac{1}{1 + \mu_-^2 B^2} \tag{3b}$$

A third quantity, which will be used later, called the magnetoambipolar quenching factor, is defined as

$$b_a = \frac{1}{1 + \mu_+ \mu_- B^2} = \frac{b_+ b_- (\mu_+ + \mu_-)}{b_+ \mu_+ + b_- \mu_-} \tag{3c}$$

The active plasma is now governed by the equations of continuity for the ions and electrons, which are given by

$$\frac{\partial n}{\partial t} = n\nu_i - \bar{\nabla} \cdot \bar{\Gamma}_{\pm} = 0 \tag{4}$$

where ν_i is the ionization frequency per electron, assumed to be constant throughout the volume. The solution for a steady-state plasma, if it exists, is obtained from Eqs. 2b, 2c, and 4, with the additional boundary condition that the density n is zero at the walls of the container, whether it is an insulator or conductor. With a container of radius R and length L, the lowest normal mode solutions for the density, currents, and electric field are:

$$n = n_o J_o\left(\frac{r}{\Lambda_r}\right) \cos\left(\frac{z}{\Lambda_z}\right) \tag{5}$$

where $\Lambda_r = R/2.405$ and $\Lambda_z = L/\pi$.

$$\bar{\Gamma}_{\pm} = \bar{i}_r \Gamma_{\pm r} + \bar{i}_z \Gamma_{\pm z} = \bar{i}_r \Gamma_{\pm R} J_1\left(\frac{r}{\Lambda_r}\right) \cos\left(\frac{z}{\Lambda_z}\right) + \bar{i}_z \Gamma_{\pm Z} J_o\left(\frac{r}{\Lambda_r}\right) \sin\left(\frac{z}{\Lambda_z}\right) \tag{6}$$

$$\bar{E} = \bar{i}_r E_r + \bar{i}_z E_z = \bar{i}_r E_R J_1\left(\frac{r}{\Lambda_r}\right) \Big/ J_o\left(\frac{r}{\Lambda_r}\right) + \bar{i}_z E_Z \tan\left(\frac{z}{\Lambda_z}\right) \tag{7}$$

Here, n_o is the density at the center of the cavity, and $\Gamma_{\pm R}$, $\Gamma_{\pm Z}$, E_R, and E_Z are the coefficients of the currents and electric field that are still undetermined and may take on a range of values. Equation 7 shows the electric field going to infinity on the boundaries, but this is not particularly troublesome, since, within a Debye length of the

wall, the sheath forms and matches the plasma to the wall.

The magnitude of the current coefficients is now determined from Eqs. 2b, 2c, and 4, by eliminating the electric field and substituting in the normal mode solutions, Eqs. 6. The result is

$$\frac{\Gamma_{\pm R}}{n_o \Lambda_r D_a} = \frac{b_a}{\Lambda_r^2} \pm \left[\frac{\nu_i}{D_a} - \frac{b_a}{\Lambda_r^2} - \frac{1}{\Lambda_z^2} \right] \frac{b_\pm (\mu_+ + \mu_-)}{\mu_\mp (b_+ - b_-)} \tag{8}$$

$$\frac{\Gamma_{\pm Z}}{n_o \Lambda_z D_a} = \frac{1}{\Lambda_z^2} \mp \left[\frac{\nu_i}{D_a} - \frac{b_a}{\Lambda_r^2} - \frac{1}{\Lambda_z^2} \right] \frac{(b_+ \mu_+ + b_- \mu_-)}{\mu_\mp (b_+ - b_-)} \tag{9}$$

where

$$D_a = \frac{\mu_+ D_- + \mu_- D_+}{\mu_+ + \mu_-}$$

It is known that the minimum value of ν_i for the maintenance of a plasma is given by

$$\frac{\nu_i}{D_a} = \frac{b_a}{\Lambda_r^2} + \frac{1}{\Lambda_z^2} \tag{10}$$

For this value of ν_i, the current coefficients are $\Gamma_{\pm R} = n_o D_a b_a / \Lambda_r$ and $\Gamma_{\pm Z} = n_o D_a / \Lambda_z$. These values are consistent with normal magnetoambipolar diffusion, and show a zero

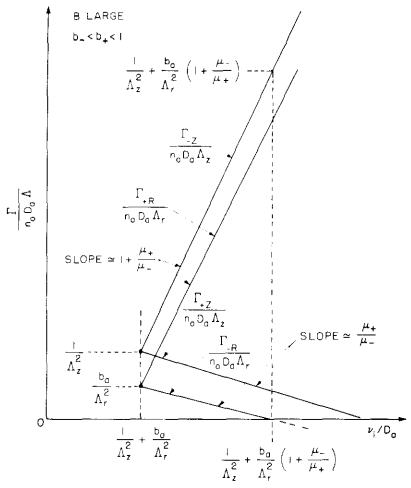

Fig. II-11. Magnetoambipolar diffusion currents.

net electric current everywhere in the plasma. As ν_i is increased, however, Eqs. 8 and 9 show that the electron and ion currents become unbalanced. A plot of these

equations is shown in Fig. II-11 for large B, where $b_- < b_+ < 1$. There are several important facts to be deduced from this plot.

(a) For insulated walls there is only one possible value of ν_i (given by Eq. 10).

(b) An increased ν_i can only be acceptable in the steady state if the walls can conduct the resultant unbalanced currents.

(c) There is a maximum value of ν_i when either Γ_{-R} (Simon limit) or Γ_{+Z} (Allis limit) goes to zero. Note that the radial currents can be adjusted because b_a is a function of B.

The physical reason for this separation of particle currents is clear. From Eq. 4, an increased ν_i calls for an increase in the divergence of both the ion and electron currents. Since the diffusion forces cannot change, the electric field must readjust to accommodate this increased current. An increase in the radial field and a decrease in the axial field allow an increase in the net current but also require that the currents be unbalanced. Solving for E_R and E_Z from Eqs. 2 and 4 shows that this is indeed the case.

Thus the solution is forced by the ionization frequency in the volume of the plasma, and the boundaries of the container play only a secondary role in accommodating the electric currents from the plasma. The changes in potential caused by the changes in the electric field will be satisfied at the walls by a readjustment of the sheath potential.

D. R. Whitehouse

References

1. A. Simon, Ambipolar diffusion in a magnetic field, Phys. Rev. 98, 317 (1955).

2. Notes on Plasma Dynamics, Summer Session, M.I.T., 1959, Section I-E (unpublished).

6. MEASUREMENT OF RADIATION FLUCTUATIONS FROM A SOURCE IN THERMAL EQUILIBRIUM

At a conference in Brussels, in 1911, Einstein (1) presented the derivation of the equation

$$\overline{(\Delta E)^2} = h\nu\bar{E}\left[1 + \frac{1}{\exp(h\nu/kT) - 1}\right] \qquad (1)$$

expressing the statistical relationship between the energy fluctuation and the mean energy of radiation in thermal equilibrium with its surroundings. Here, T is the absolute temperature, h is Planck's constant, k is Boltzmann's constant, and ν is the spectral frequency of the radiation. The fluctuation in the number of photons in the

ensemble is obtained by dividing Eq. 1 by $(h\nu)^2$:

$$\overline{(\Delta N)^2} = \bar{N}\left[1 + \frac{1}{\exp(h\nu/kT) - 1}\right] \tag{2}$$

This can be rewritten as

$$\overline{(\Delta N)^2} = \bar{N}\left[1 + \frac{N}{g}\right] \tag{3}$$

where g is the number of cells in the volume of phase space occupied by the N photons. The quantity N^2/g, to the author's knowledge, has never been measured for a radiant source in thermal equilibrium, although Hanbury Brown and Twiss (2), Rebka and Pound (3), and Brannen, Ferguson, and Wehlau (4) have measured the term for various high-temperature sources for which an equilibrium temperature could not be defined.

One might think that in the fifty years since the derivation of Eq. 1 attempts would have been made to verify it. However, serious experimental difficulties arise in measuring the quantity $\bar{N}^2/g$. The radiant source cannot be hotter than approximately 3000°K because laboratory sources do not exist in thermal equilibrium at higher temperatures. At 3000°K, $\bar{N}/g \approx 10^{-3}$ in the visible part of the spectrum and is smaller toward the ultraviolet. Hence the fluctuation term $\bar{N}^2/g$, predicted by classical wave theory, is largely masked by the shot-noise fluctuation, $\bar{N}$. At long wavelengths, the classical fluctuation predominates, but the power emitted by a black-body radiator at these wavelengths is so small that the fluctuation power is much smaller than the detector noise. In order to detect the classical fluctuation term in the presence of other noises, we have to resort to special electronic techniques.

1. The Experiment

Light from an incandescent tungsten filament S (Fig. II-12) passes through an infrared transmitting filter F and is incident on a half-silvered mirror (HSM). The reflected light falls on a lead sulfide detector D_1, while the transmitted light is incident on D_2. The output signals of the two detectors are electronically correlated (Fig. II-13). Purcell (5) has shown that the crosscorrelation, $\overline{\Delta N_1 \Delta N_2}$, in the number of photons incident on two detectors D_1, D_2 is equal to one-fourth of the fluctuation, $\overline{(\Delta N)^2}$, in the beam that would be incident on D_2 in the absence of the half-silvered mirror.

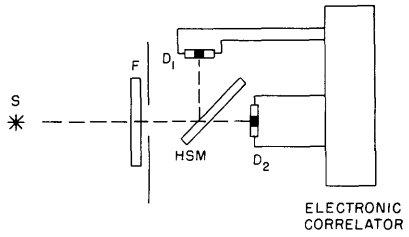

Fig. II-12. Diagram of optical system illustrating intensity interferometry.

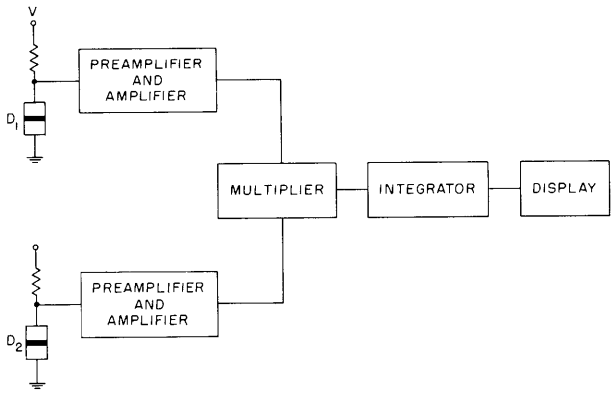

Fig. II-13. Two-detector correlation system.

Thus, by electronically crosscorrelating the output of the two detectors, the fluctuation in the radiation from source S can be determined.

The advantage of the correlation technique can be understood by considering two detectors that receive identical signals s, and independent noises n_1 and n_2. When the two detector output signals are electronically multiplied, we obtain the product

$$(s+n_1)(s+n_2) = s^2 + sn_1 + sn_2 + n_1n_2 \tag{4}$$

Here the first term s^2 is always positive. The other terms are positive or negative in some random sequence. If expression 4 is integrated over a long period of time T, these random terms average to zero, and the integral is dominated by the term s^2. If the system has a response time τ, the correlator output signal S will be s^2T/τ. The noise $\underline{N}$ in the correlator output is given by $n_1n_2(T/\tau)^{1/2}$, if $s \ll n_1, n_2$. Let $n_1 = n_2 \equiv n$, then the correlator output signal-to-noise ratio is

$$\frac{S}{\underline{N}} = \frac{s^2}{n^2}\left(\frac{T}{\tau}\right)^{1/2} \tag{5}$$

For a derivation of this equation see Lee, Cheatham, and Wiesner (6), or Goldstein (7).

In the present experiment, the quantity s^2 corresponds to the expected crosscorrelation $\overline{\Delta N_1 \Delta N_2}$, modified appropriately by detector-response and amplifier-gain terms. The noise terms n, measured by means of a voltmeter, gave an expected ratio s^2/n^2 of approximately 10^{-3}. The system response time τ was determined by the cooled lead sulfide time constant of approximately 1 msec, so that the time T that is required to achieve a correlator output signal-to-noise ratio of unity was approximately 1000 sec.

With the use of a variety of different optical systems, a number of correlation runs were made, in which T varied from 10 min to 240 min. In a typical set of runs, the expected correlation was determined by using Eq. 6. (The resulting expression is

similar to that obtained by Hanbury Brown and Twiss, whose wave theoretical results are in agreement with Eq. 3.)

$$S = 0.4\left[V_1 V_2 \gamma_1 \gamma_2 \delta_1 \delta_2 \int |F(f)|^2 \, df \, \Delta\nu^{-1} \beta \Gamma T\right] \tag{6}$$

in which

0.4	= a parameter of the correlator
$V_1 V_2 = 0.422\ V^2$	= the product of the detector bias voltages
$\gamma_1 \gamma_2 = 0.015$	= the product of the detector-response terms
$\delta_1 \delta_2 = 0.18$	= the product of the impedance-matching terms at the amplifier inputs
$\int \lvert F(f)\rvert^2 \, df = 2.4 \times 10^{14}\ \text{sec}^{-1}$	= the integrated product of amplifier gain
$\Delta\nu = 9 \times 10^{12}\ \text{sec}^{-1}$	= a measure of the spectral-radiation bandwidth
$\beta = 1.04$	= a measure of the source polarization, which is unity for completely unpolarized light; 2 for completely polarized light
$\Gamma = 0.89$	= a coherence factor that lies between zero and unity
$T = 14,400$ sec	

For S, we obtain $160 \pm 80\ V^2$ sec. The measured value was $220 \pm 373\ V^2$ sec. The possible error in the predicted value is largely the result of the uncertainty in the detector time constant, and the uncertainty in the measured value is the result of the scatter of the integral sampled at 480 points during the integration.

Ten experimental runs were made; the results were in agreement with the predicted values, within the limits of the experimental error. The signal-to-noise ratio of all of the integrations taken together was 3.9. The probability of accidentally obtaining such a high signal-to-noise ratio is less than 10^{-4}.

A detailed discussion of the experiment can be found in the author's thesis (8).

M. O. Harwit

References

1. A. Einstein, Rapport sur l'état actuel du problème des chaleurs specifiques, La Théorie du Rayonnement et les Quanta (Gauthier-Villars, Paris, 1912), pp. 407-435.

2. R. Hanbury Brown and R. Q. Twiss, Proc. Roy. Soc. A242, 300 (1957); A243, 291 (1958); A248, 199 (1958); A248, 222 (1958).

3. G. Rebka and R. V. Pound, Nature 180, 1035 (1958).

4. E. Brannen, H. S. I. Ferguson, and H. Wehlau, Can. J. Phys. 36, 871 (1958).

5. E. M. Purcell, Nature 178, 1449 (1956).

6. Y. W. Lee, T. P. Cheatham, and J. B. Wiesner, Proc. IRE 38, 1165 (1950).

7. S. Goldstein, Proc. IRE 43, 1663 (1955).

8. M. O. Harwit, Measurement of Fluctuations in Radiation from a Source in Thermal Equilibrium, Ph.D. Thesis, Department of Physics, M.I.T., March 2, 1960.

B. PLASMA ELECTRONICS*

Prof. L. D. Smullin
Prof. H. A. Haus
Prof. A. Bers
Prof. D. J. Rose
K. Arons
P. Chorney
T. J. Fessenden
W. D. Getty
W. Larrabee
L. M. Lidsky
A. Peskoff
B. Reiffen
C. W. Rook
S. D. Rothleder
W. C. Schwab
D. V. Turnquist

1. A LOW-PRESSURE GAS-ARC DEVICE

In Quarterly Progress Report No. 56, a proposal was made for generating a highly ionized plasma with a high-current, low-pressure gas arc (1). This device was constructed and has been operated. In this report we shall describe the main features of the apparatus and the operating characteristics observed during the short period since its construction was completed. A more detailed description of the operating characteristics of the same type of arc has been given by Michelson and Rose (2).

The vacuum chamber of the gas arc (Fig. II-14) is essentially a cylinder, 53 inches long, and with an inside diameter of 4 inches. The center section is a 4-way brass cross, and the two end sections are Pyrex T-sections. The short arm of the center cross leads to a vacuum-pump port in the rear, and to the viewing port in front. The glass T-sections in the long arm also connect the chamber to two other vacuum-pump ports. At the present time, two 4-inch oil diffusion pumps are used with a single, 15-cfm forepump. Each vacuum-pump port can be closed with a straight-through gate valve so that the chamber can be opened and re-evacuated without turning off the diffusion pumps. This pumping system will maintain a pressure of approximately 10^{-3} mm Hg when the arc is operating, and 10^{-6} mm Hg when it is not.

Water-cooled brass electrode holders (1.375 inches O.D., and 43 inches long) are inserted in the vacuum chamber from each end of the long cylinder. These rods go through O-ring seals, to permit adjustment of the arc length while the system is being evacuated. The anode is a short cylinder of solid copper mounted on the tip of one of the rods. The cathode, made of reactor-grade carbon, is mounted on the other rod (Fig. II-15). When the arc is operating, argon gas flows through the rod and the axial hole in the cathode into the vacuum chamber.

The electromagnets are mounted coaxially with the long arm of the cross, as near the center as possible. Each magnet has 1600 turns and is water-cooled. They can produce a total field in excess of 500 gauss along the arc.

Initial attempts to obtain a stable arc were not successful because the input gas flow was apparently too small to support a gas arc. With a very small gas flow the arc would run between an intensely bright hot spot on the face of the cathode, and a similar

---

*This work was supported in part by National Science Foundation under Grant G-9930.

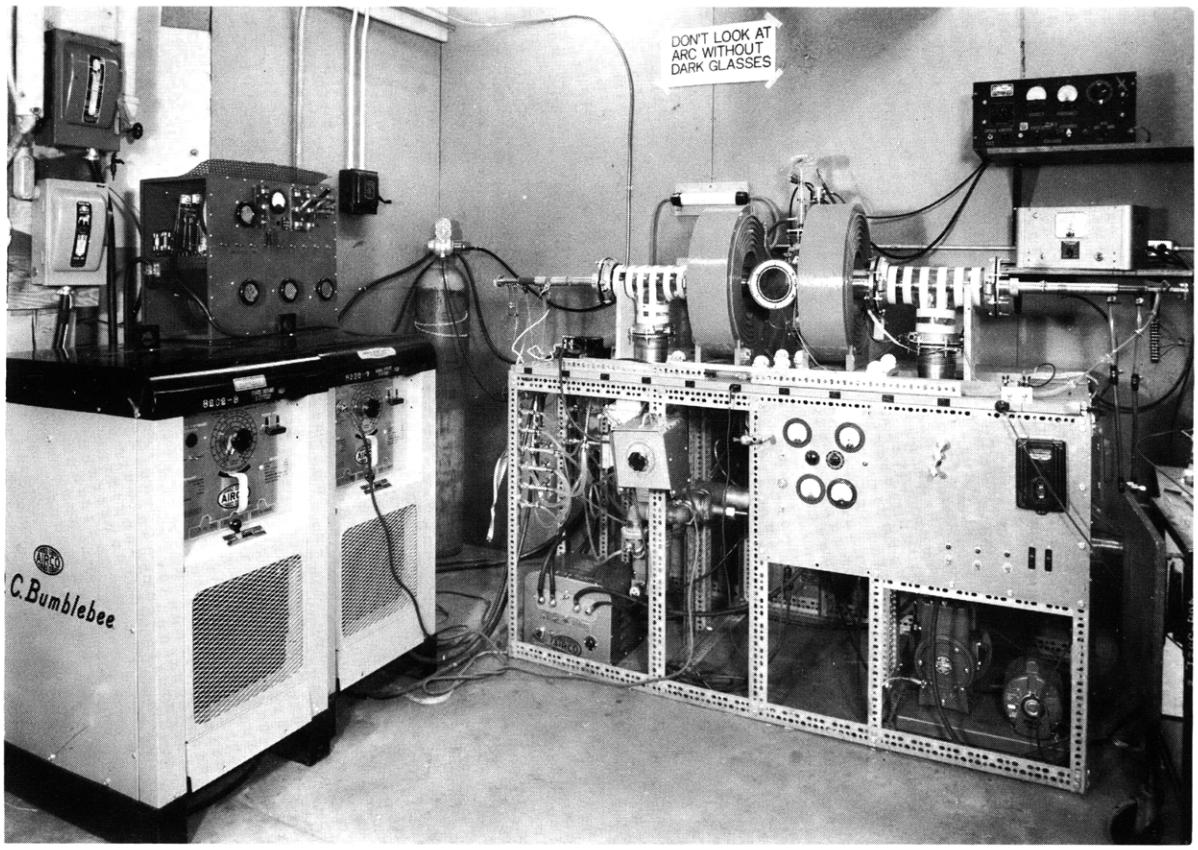

Fig. II-14. Gas-arc apparatus.

hot spot on the anode. In this mode of operation, the carbon cathode eroded very rapidly. With an increased flow of argon the arc becomes very stable, and appears to originate from inside the axial hole in the cathode. As soon as the arc enters the hole, the whole end of the cathode becomes incandescent, and the rate of erosion of carbon decreases noticeably. The arc will remain in this mode of operation for several minutes, at which time the tip of the cathode burns off. During the period of stable operation, the arc current and voltage are relatively steady.

We have operated the arc with currents in the range 35-90 amp. The arc will apparently carry a larger current, but it will extinguish if the current is reduced below a minimum value that depends roughly on the diameter of the cathode tip. When the 0.25-inch tip burns off, the arc will run from the 0.125-inch diameter stub at lower currents. The voltage varied between 30-60 volts over this range of current. We have found that the rate of gas input must be carefully adjusted to obtain a stable arc. A minimum flow, for which the pressure is approximately 10^{-3} mm Hg, is necessary to support a stable arc. A flowmeter is being installed to measure the rate of gas flow directly.

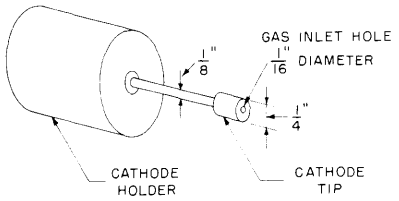

Fig. II-15. Cathode of the gas arc.

Our experience in operating the gas arc has indicated that it will be necessary to increase the pumping speed of our system in order to maintain the required pressure for electron-beam experiments in this device. Several possibilities for decreasing the operating pressure are being investigated. Experiments are also planned for measuring the electron density and temperature in the arc by microwave techniques. Our immediate efforts will be directed toward learning how to run the arc in its stable mode for uninterrupted periods of 10-15 minutes.

W. D. Getty

References

1. L. D. Smullin and W. D. Getty, Electron-beam stimulated plasma oscillation, Quarterly Progress Report No. 56, Research Laboratory of Electronics, M.I.T., Jan. 15, 1960, pp. 27-34.

2. C. Michelson, A type of hollow-cathode discharge, and D. J. Rose, Analysis of a cavity cathode discharge in carbon, ONRL-2802, Thermonuclear Project Semiannual Report for period ending July 31, 1959, Oak Ridge National Laboratory, pp. 54-58; 59-65.

2. PROPAGATION IN PLASMA WAVEGUIDES

In Quarterly Progress Report No. 56, we were concerned with the effect of the positive ions on the propagation characteristics of plasma waveguides (1). The problem was formulated on a quasi-static basis (2)(that is, the analysis is valid as long as the propagation constant $\beta_z \gg k$, where $k = \omega/c$), and collisions were ignored. (The effect of collisions is now being studied and will be reported on in a future report.) We gave expressions from which the dispersion relations for the propagation of radially symmetric modes in a radially symmetric waveguide may be calculated. The special case of the plasma-filled waveguide was discussed.

For the partially filled waveguide ($b \neq a$), the qualitative behavior is much the same as that of the completely filled waveguide for the higher-order radial modes. For the lowest-order radial mode, the surface wave now appears within limited frequency bands, as shown in Figs. II-16 and II-17. When $\omega_{pe} > \omega_{ce}$, a low-frequency and a high-frequency

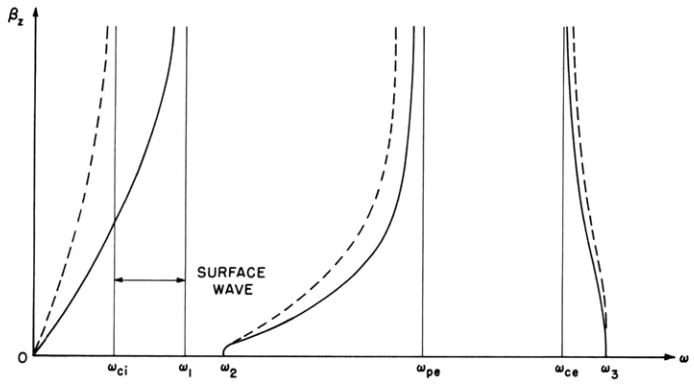

Fig. II-16. Dispersion characteristic of partially filled plasma waveguide for $\omega_{ce} > \omega_{pe}$. Solid lines indicate the lowest-order radially symmetric mode; broken lines indicate a higher-order radially symmetric mode.

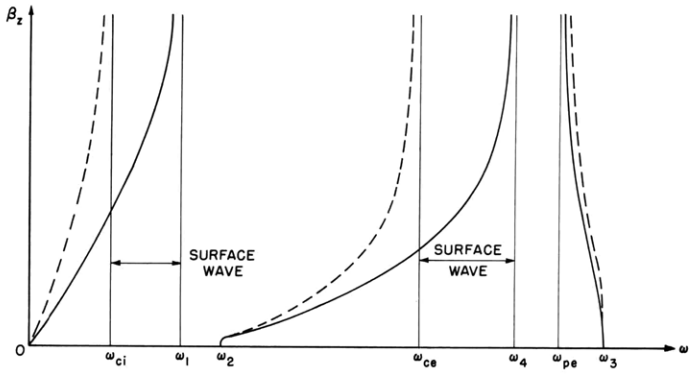

Fig. II-17. Dispersion characteristic of partially filled plasma waveguide for $\omega_{pe} > \omega_{ce}$.

surface wave appear; but for $\omega_{pe} < \omega_{ce}$, only a low-frequency surface wave appears. When we consider the effect of the ions negligible as compared with the effect of the electrons for frequencies much higher than ω_{pi} and ω_{ci}, we find that the high-frequency surface wave is still the same as that previously described (3, 4, 5). The low-frequency surface wave propagates for $\omega_{ci} < \omega < \omega_1$, where ω_1 is very close to ω_2 (which is defined below). It is given approximately by

$$\omega_1 = \omega_2 \left(1 - \frac{\omega_{pi}^2}{\omega_{pe}^2} \frac{1 + \left(\omega_{pe}^4 / \omega_{ce}^4 \right)}{\left(1 + \omega_{pe}^2 / \omega_{ce}^2 \right)^2} \right)^{1/2}$$

The poles and zeros of β_z for the higher-order radial modes occur at the same

frequencies as in the completely filled waveguide. Those for the lowest-order radial mode occur as indicated in Figs. II-16 and II-17. The other critical frequencies referred to in these figures are given by

$$\omega_2 = \left(\omega_{ci}^2 + \frac{\omega_{pi}^2}{1 + \left(\omega_{pe}^2 / \omega_{ce}^2 \right)} \right)^{1/2}$$

$$\omega_3 = \left(\omega_{pe}^2 + \omega_{ce}^2 \right)^{1/2}$$

$$\omega_4 = \left(\frac{\omega_{pe}^2 + \omega_{ce}^2}{2} \right)^{1/2}$$

These sketches are intended to give only a qualitative idea of the dispersion characteristics. The frequencies indicated are intentionally not to scale, for the sake of convenience. However, we must keep in mind that ordinarily the frequency spread between the ion quantities and the electron quantities is a few orders of magnitude; for instance, when we have a neutral plasma with singly charged ions, $\omega_{pe}/\omega_{pi} = (m_i/m_e)^{1/2}$ and $\omega_{ce}/\omega_{ci} = m_i/m_e$. These large differences were used to great advantage in determining the propagation characteristics.

P. Chorney

References

1. P. Chorney, Propagation in plasma waveguides, Quarterly Progress Report No. 56, Research Laboratory of Electronics, M.I.T., Jan. 15, 1960, pp. 39-41.

2. P. Chorney, Approximate field solutions, Quarterly Progress Report No. 52, Research Laboratory of Electronics, M.I.T., Jan. 15, 1959, pp. 47-49.

3. P. Chorney, Electron-Stimulated Ion Oscillations, Technical Report 277, Research Laboratory of Electronics, M.I.T., May 26, 1958.

4. L. D. Smullin and P. Chorney, Propagation in ion-loaded waveguides, Proc. Symposium on Electronic Waveguides, Polytechnic Institute of Brooklyn, New York, April 1958.

5. A. W. Trivelpiece, Slow-Wave Propagation in Plasma Waveguides, Technical Report No. 7, Electron Tube and Microwave Laboratory, California Institute of Technology, May 1958.

C. PLASMA MAGNETOHYDRODYNAMICS AND ENERGY CONVERSION*

Prof. O. K. Mawardi
Prof. H. H. Woodson
Prof. J. A. Fay
Prof. W. D. Jackson
Prof. D. C. Pridmore-Brown
Dr. R. Gajewski†
T. I. Sundstrom

A. W. Angelbeck
G. W. Bukow
L. Y. Cooper
D. M. Dix
D. A. East
W. H. Heiser

G. B. Kliman
A. T. Lewis
J. K. Oddson
J. P. Penhune
J. W. Poduska
K-F. Voyenli
B. Zauderer

1. HYDROMAGNETIC RESONATORS

The behavior of hydromagnetic waves in a cylindrical resonator of arbitrary cross section with a magnetic field applied in a direction parallel to the generators of the cylinder has been examined. The eigenfrequency spectrum for all possible modes and types of wave has also been derived. It is shown that a transverse longitudinal acoustic (TLA) type of wave when reflected from a rigid conducting termination generates an accompanying transverse longitudinal magnetohydrodynamic (TLM) type of wave, and vice versa. Energy losses resulting from the finite viscosity and electric conductivity of the fluid, as well as from the finite conductivity of the walls, are then estimated for a purely transverse (T) type of wave. A Q-factor for the T wave is subsequently calculated.

A paper on the work described here has been submitted for publication.

R. Gajewski, O. K. Mawardi

2. STUDY OF A MAGNETIC PROBE

Investigation of the flow about a magnetic probe (search coil) placed in a shock tube has been initiated. The basic principle of operation of such a probe is well known; the object of our investigation is to determine the field distortion created by the probe, and hence fix the range of the significant parameters within which the probe readings can be regarded with some degree of confidence.

The major inherent sources of error in the use of the probe arise from two causes: (a) distortion of the field because of the flow interruption; and (b) ablation of the probe casing. The first effect is due to the fact that the magnetic field present in the plasma is reluctant to diffuse out; hence, since the probe excludes the plasma from a certain region of space, it tends also to exclude the magnetic field from the same region. The second effect is due to the fact that the high plasma temperatures will cause the probe

---

*This work was supported in part by National Science Foundation under Grant G-9930; and in part by Contract AF19(604)-4551 with Air Force Cambridge Research Center.

†Sloan Foreign Postdoctoral Fellow, from the Institute for Nuclear Research, Warsaw, Poland.

casing to ablate, and even ionize; thus a conducting shield is created about the probe surface. In the present applications, it is believed that the first effect is the more significant because the test time is extremely short, and thus ablation is prevented; and also because an ionized layer about the probe would not be of any greater electric conductivity than the plasma proper.

The usual boundary-layer arguments can be applied to the hydromagnetic flow (if we assume that the probe has the shape of a flat plate), and the following results can be deduced: The boundary layer grows, in the usual fashion, away from the leading edge, but further downstream it tends to a constant value. In the region near the leading edge (but slightly away from it), the boundary layer thickness is given by

$$\frac{\delta}{L} \frac{1}{\sqrt{R_e}}$$

and the change in the normal component of the field is given by

$$\Delta B_n \sim \frac{R_m}{R_e}$$

Further downstream, where the inertial forces become negligible, the boundary-layer thickness is given by

$$\frac{\delta}{L} \sim \frac{M_m}{(R_e R_m)^{1/2}}$$

where M is the dimensionless Alfvèn speed. In this case the change in the normal component of the magnetic field is given by

$$\Delta B_n \sim \frac{M_m^2}{R_e}$$

Thus, downstream, the boundary-layer thickness is independent of L, the distance along the plate, and the change in the normal component of the field goes to zero. Near the tip, however, the change in the normal component is of the order of the ratio of the magnetic Reynolds number to the viscous Reynolds number; this ratio can be as high as unity in shock tube applications.

Another factor of considerable importance is the transient response of the probe; both this problem and the steady-state problem are being attacked in a highly idealized theoretical manner. It is believed that the results of this analysis will yield a great deal of information concerning the qualitative and quantitative character of the flow.

Some preliminary experiments with the probe used in a shock tube have been performed. It has been found that the peak signals obtained from the probe are of the same

Fig. II-18. Retouched photograph of a signal detected by the probe.

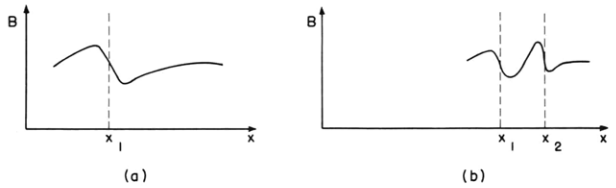

Fig. II-19. Idealized representation of magnetic field distribution: (a) before shock formation; (b) after shock formation.

order of magnitude as those expected from theoretical considerations. A signal (retouched) is shown in Fig. II-18. The first dip in the signal is attributed to the fringing of the field behind the shock, as previously explained (1). The sharp rise is the passage of the shock proper. The sudden dip in the signal which follows the shock has not been completely explained. A tentative explanation is as follows: The discharge current produces a magnetic field that opposes the initial applied magnetic field. Immediately after the discharge, this magnetic field is not well confined by the circuitry leading to the electrodes, and hence fringing is large. The magnetic field distribution before the shock forms is as shown in Fig. II-19a. The discharge current is at x_1. As the current sheet progresses down the tube, a shock is formed by compression waves generated at the sheet. Since each such wave will increase the magnetic field strength by essentially the same amount, at some later time, after the shock is formed, the field distribution will be as shown in Fig. II-19b. The shock is at x_2, and the current sheet at x_1.

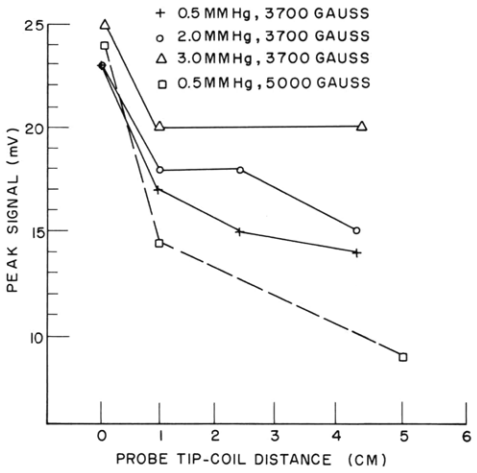

Fig. II-20. Maximum strength of magnetic field behind the shock under different experimental conditions.

Some experimental evaluations of the probe signals have been performed by varying the distance from the search coil to the tip of its protective casing. The major effect of increasing this distance is that of attenuating the peak signal. The results of a series of such experiments are shown in Fig. II-20. There are several points of interest in connection with these results. First, it is seen that the distortion of the magnetic field is confined to the region near the tip of the probe; this is in accord with the dimensional arguments that were presented. Second, as the initial pressure is increased, the field distortion is lessened; this is also in accord with our dimensional arguments, since an increase in initial pressure reduces the ratio R_m/R_e. Finally, as the initial magnetic field strength is increased, the distortion of the field by the probe is increased. This distortion results from increasing the ratio R_m/R_e.

D. M. Dix, O. K. Mawardi

References

1. Z. J. J. Stekly and O. K. Mawardi, Hydromagnetic shocks, Quarterly Progress Report No. 55, Research Laboratory of Electronics, M.I.T., Oct. 15, 1959, pp. 42-47.

3. MAGNETOHYDRODYNAMIC INTERACTIONS IN SEEDED DETONATION WAVES*

Experiments were performed to determine the maximum electric power that can be generated by passing an ionized gas through a magnetic field. The equipment consisted of a vertical detonation tube filled with a 50-50 oxyacetylene mixture at an initial pressure of 0.1 atmosphere and seeded with a 0.01-0.1 mol fraction of potassium acetylide. A detonation wave was initiated by a spark plug at the top of the tube. The gas behind the wave reached a speed of 1300 meters per second, and a peak conductivity of 2.7 mhos/cm. The gas is in thermodynamic equilibrium for approximately 100 μsec, with a pressure of 4 atmospheres and a temperature of 3500°K.

This slug of gas is then passed through a crossed electric and magnetic field (as shown in Fig. II-21). The magnetic field of 10,000 gauss is perpendicular to the gas velocity vector. The electric-field vector, which is mutually perpendicular to both the velocity and magnetic field, is produced by two 6-cm^2 plane copper electrodes, spaced 4 cm apart and connected to an external load of variable resistance.

The amount of power that the gas can generate is given by

$$P = J \cdot E = \sigma(E+V\times B) \cdot E$$

where J is the current density, E is the external electric field applied at the electrodes,

*This work is sponsored in part by the Office of Naval Research through Project SQUID, Phase III, under contract with Massachusetts Institute of Technology.

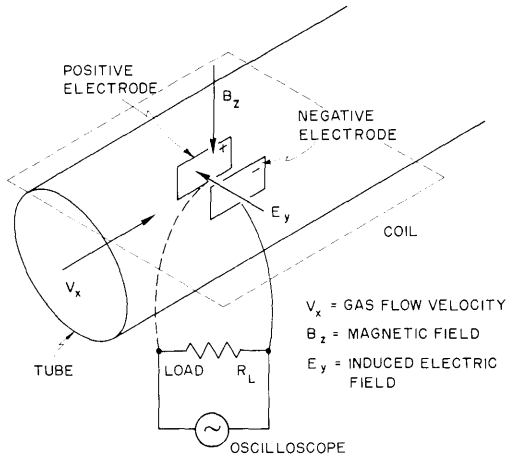

Fig. II-21. Schematic diagram of test region. The electrodes are on the inside walls, diagonally opposite each other, and parallel to the sides of the coil.

V is the gas velocity, B is the magnetic field, and σ is the gas conductivity. All units are rationalized mks units.

The gas velocity is fixed by the strength of the detonation wave. Therefore, for given magnetic and electric (external load) fields, the power should be a function of the gas conductivity. For the parameters in this experiment, the maximum value of the current can be obtained by short-circuiting the electrodes. It is approximately 30 amps/cm^2. The electrodes will have sheaths formed on their surfaces. The maximum current that can be passed through the sheath is the random ion current:

$$J_p = \frac{n \bar{c} e}{4}$$

where n is the ion density, $\bar{c}$ is the thermal velocity with the assumption of a Maxwellian velocity distribution, and e is the ionic charge. For the seeded gas, this current is approximately 50 amps/cm^2. Therefore, by doubling the magnetic field it should be possible to obtain this current. However, at 20,000 gauss, the cyclotron frequency, ω, of the electrons equals the collision frequency, ν, and this produces a drift (Hall) current in the direction of the gas velocity vector and reduces the net current to the electrodes by a factor of $\frac{1}{1 + \left(\frac{\omega}{\nu}\right)^2}$.

The plasma sheath is a Debye length (10^{-5} cm for this gas) thick. However, there is a boundary layer on the electrode which is given by $\delta = (\lambda x)^{1/2}$, where λ is the mean-free path, and x is the length of the electrode. This boundary layer is many orders of magnitude thicker than the plasma sheath. It will therefore govern the amount of current flow to the electrodes. The current through the boundary layer flows by

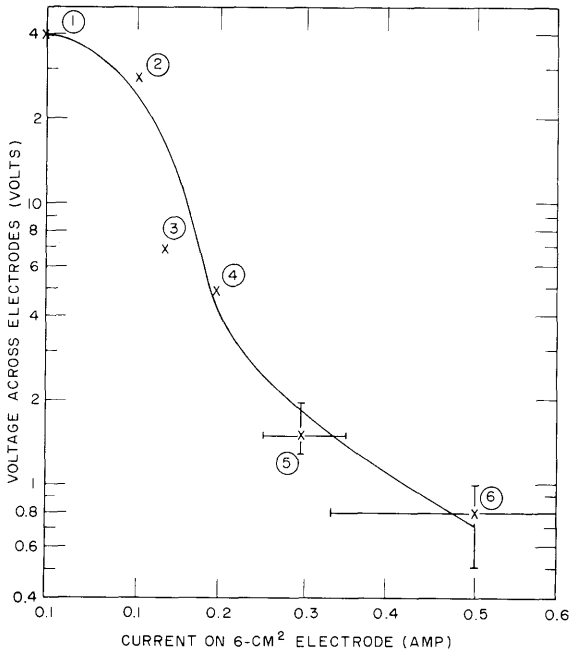

Fig. II-22. External voltage across the electrodes as a function of output current.

ambipolar diffusion. It is given by $J = \frac{D_a}{\delta} ne$ amps/cm^2, where D_a is the ambipolar diffusion coefficient. For the gas in this experiment, it is approximately 0.25 amp/cm^2. This is the order of magnitude that was obtained in this experiment. Figure II-22 is a plot of the experimental points obtained. The open-circuit voltage is 40 volts. As the external load was decreased, the current flow increased slightly, which indicates that the boundary layer presented a constant nonlinear impedance in the circuit, irrespective of the external load. The higher values of the current are very inaccurate.

J. A. Fay, B. Zauderer

References

1. S. Basu, Ionization in Seeded Detonation Waves, Sc.D. Thesis, Department of Mechanical Engineering, M.I.T., September 1959.

2. B. Zauderer, Magnetohydrodynamic Interactions in Seeded Detonation Waves, S.M. Thesis, Department of Mechanical Engineering, M.I.T., 1960.